

## Wave function orthogonality in coupled-channel systems

Q. Haider\* and J. T. Londergan

*Department of Physics, Indiana University, Bloomington, Indiana 47405*

(Received 21 July 1980)

Recent work by Noble and collaborators has pointed out that wave function orthogonality in bound-state to continuum-state transitions can produce large cancellations in transition amplitudes. In single-channel examples, nonorthogonal wave functions (such as plane waves) were shown to greatly overestimate the exact results even at high energies. In this paper we examine a simple coupled-channel model which can be exactly solved for the many-channel scattering and bound wave functions. In such a model, the exact transition amplitude can be compared with standard plane-wave and distorted-wave approximations. Dispersive corrections are shown to be large and to persist even at high energies.

[NUCLEAR REACTIONS Orthogonality constraints on bound-continuum transitions in coupled-channel systems. Dispersive corrections to DWIA.]

### I. INTRODUCTION

There have been several experiments carried out recently which have the capability of probing high-momentum components of nuclear single-particle wave functions. Among these are bound state to continuum state knockout processes involving absorption of a photon or meson, such as  $A(\pi, N)B$  (Ref. 1) or  $A(\gamma, N)B$  (Ref. 2) at intermediate energies. These reactions are promising areas for studying the effects of exchange-current phenomena in nuclei or multistep reaction mechanisms, and also for probing components of single-particle wave functions at large momentum. However, there are long-standing questions regarding the importance of wave function orthogonality in these reactions.<sup>3-5</sup> The orthogonality question arises since the absorption (or emission) of a particle changes the energy of the nucleus. For absorption reactions, the initial (bound) and final (continuum) nuclear states are eigenfunctions of the nuclear Hamiltonian at different energies and are orthogonal; i. e., if we denote the initial and final nuclear wave functions as  $\psi_i$  and  $\psi_f$ , respectively, then the wave functions must satisfy

$$\langle \psi_f | \psi_i \rangle = \delta_{fi}. \quad (1.1)$$

Standard distorted-wave treatments of these reactions (which evaluate the interaction of the ejected nucleon via a complex and energy-dependent optical potential) will produce wave functions which do not manifestly satisfy the orthogonality criterion. It would be useful to have estimates of the importance of orthogonality in these reactions, in order to appreciate the magnitude of this problem in medium-energy reactions. Recent work by Noble and collaborators<sup>5</sup> has been very useful in this regard. Using flux conservation techniques to explicitly account for orthogonality in the nuclear

wave functions, Noble has been able to provide equations for calculating knockout amplitudes, and in certain cases he is able to compare the "correct" amplitudes with amplitudes calculated using plane waves for the ejected nucleon.

These results are interesting because they point out three features of knockout reactions and orthogonality: (1) the difference between plane-wave amplitudes and results calculated using Noble's techniques is quite large (plane-wave amplitudes greatly overestimate the exact result); (2) the large differences persist even at high energies, where it is often asserted that plane waves should give progressively better fits to the correct amplitudes; (3) the amplitudes are very model-dependent (since two different approximations by Noble give rise to answers which differ asymptotically by a factor of 2). Noble wrote down the full coupled-channel amplitude for knockout reactions, but he used examples where both the binding and scattering of the single nucleon were governed by the same real potential  $V$ , a fact which made it easier to employ the flux-conservation arguments he set forth.

Although the estimates obtained by Noble were very useful in showing the possible effects of orthogonality, this does not necessarily imply that large orthogonality modifications will be necessary to correct "traditional" nuclear physics calculations of knockout reactions—by traditional, we mean calculations which include the nucleon-nucleus interaction via a complex and energy-dependent optical potential, and which use a spectroscopic factor for the single-particle bound wave function. As is well known, one distinctive feature of nucleon-nucleus reactions at intermediate energies is the strong coupling of different nuclear states in the reaction. Consequently, if we are looking at, say,  $(\gamma, p)$  reactions on an  $A$ -body target leading to a specific final state in the  $(A-1)$  body residual

nucleus, then the final-state interaction of the proton with the residual nucleus must take into account the effects of a large number of states of the  $(A-1)$  body system. The explicit energy dependence of the proton-nucleus effective interaction results from reducing the many-channel nuclear system to an equivalent one channel problem with an (energy-dependent) effective interaction, as was shown by Feshbach.<sup>6</sup> The spectroscopic factor for the bound state single-particle wave function also accounts for some features of the strong channel coupling by renormalizing the proton-nucleus wave function to account for strength in the other channels.

Since the nuclear system is characterized by strong coupling to intermediate excited nuclear states, it is not clear that the results obtained by Noble from a one-channel description of the bound and scattering states will be applicable for realistic situations. For example, one could imagine a situation where plane-wave calculations might dramatically overestimate the "exact" result, but where standard distorted-wave methods give very good agreement with the correct amplitude. In this paper, we present the results of a model calculation where we can examine knockout reactions in a coupled-channel system. In this model, we have a nucleon interacting via separable interactions with a nuclear core possessing a ground state and a single internal excitation, and we calculate the amplitude for a transition where the initial bound state of the nucleon plus core absorbs a scalar meson, going to a final state consisting of a continuum nucleon and the ground state of the nuclear core.

Such a model is useful because we can analytically solve the coupled-channel problem for the bound and scattering states of the nucleon relative to the core. Thus, we can solve the multichannel nuclear problem while explicitly maintaining orthogonality. For purposes of illustration, we will choose a simple form for the absorption operator for the "meson"; in this case, the resulting amplitude can be shown to consist of three terms. The first term is just the plane-wave impulse approximation (PWIA) for the knockout reaction; including the second term gives the distorted-wave impulse approximation (DWIA) for the reaction with a spectroscopic factor for the bound proton; the third term provides an additional dispersive contribution not included in standard distorted-wave analyses. In the context of this model, we will examine the following questions:

- (1) To what extent is the DWIA analysis an adequate representation of the full amplitude?
- (2) Do Noble's estimates of the importance of orthogonality corrections (based on single-channel

examples) overestimate the effects of such corrections in many-channel systems?

- (3) How large are the dispersive corrections, and does their importance diminish with increasing energy?

In Sec. II, we review the formalism for calculating knockout reactions in coupled systems and we repeat the arguments by Noble which led to his estimates of the effects of orthogonality corrections in coupled systems. In Sec. III, we present the coupled separable potential model which we have employed for the nuclear wave functions. We write down the solutions for the wave functions and we show phase shifts for three different cases which we use as examples. Details of these equations are deferred to Appendix A. In Sec. IV we present the exact results of our calculations and compare with PWIA and DWIA predictions, and with Noble's estimates extrapolated from one channel systems; we also present our conclusions based on this work.

## II. COUPLED SYSTEMS AND NUCLEAR REACTIONS

For the purpose of illustration, we shall consider reactions of the form  $A(\pi, N)B$  or  $A(\gamma, N)B$  in this paper. Also, wherever convenient we will follow the notation used by Noble.<sup>5</sup> We consider the residual nucleus  $|B\rangle$  to have an orthogonal set of intrinsic excited states  $|n\rangle$ , and we divide the total Hamiltonian  $\mathcal{K}$  into an intrinsic term  $\mathcal{K}_{\text{int}}$  and a one-particle term relative to the intrinsic states, i. e. ,

$$\mathcal{K} = -\nabla^2/2M + V + \mathcal{K}_{\text{int}}. \quad (2.1)$$

In Eq. (2.1), the states  $|n\rangle$  are eigenstates of  $\mathcal{K}_{\text{int}}$  with eigenvalues  $\epsilon_n$ ,

$$\mathcal{K}_{\text{int}}|n\rangle = \epsilon_n|n\rangle, \quad (2.2)$$

and the potential  $V$  is a matrix which couples the single nucleon to various intrinsic states; it will turn out to be most useful to expand in terms of single-particle momentum components of the wave functions

$$\langle \vec{p} | \psi_i \rangle = \sum_n \psi_n(\vec{p}) |n\rangle, \quad (2.3)$$

$$\langle \psi_f | \vec{p} \rangle = \sum_n \langle n | \psi_n^{(-)*}(\vec{p}).$$

In Eq. (2.3),  $\psi_n(\vec{p})$  are single-particle components of the initial bound state wave function  $|A\rangle$ , and  $\psi_n^{(-)*}(\vec{p})$  are scattering wave functions whose precise form is determined by the boundary conditions for a particular reaction. With this expansion, the statement of orthogonality for the initial and final states is

$$\langle \Psi_f | \Psi_i \rangle = \int \frac{d^3p}{(2\pi)^3} \sum_n \psi_n^{(-)*}(\vec{p}) \psi_n(\vec{p}) = 0. \quad (2.4)$$

The transition matrix element for absorbing a boson of momentum  $\vec{k}$  can be written as

$$T_{fi}(\vec{k}) = \sum_n \int \frac{d^3\vec{p}}{(2\pi)^3} \psi_n^{(-)*}(\vec{k} + \vec{p}) O \psi_n(\vec{p}) \\ + \sum_{n,n'} \int \frac{d^3\vec{p}}{(2\pi)^3} \psi_n^{(-)*}(\vec{k} + \vec{p}) F_{nn'}(\vec{k}) \psi_n(\vec{p}). \quad (2.5)$$

The operator  $T_{fi}$  contains two parts: the first part involves absorption of the boson by a nucleon, governed by the transition operator  $O$ . The second part [given by the form factor  $F_{nn'}(\vec{k})$ ] contains two types of terms: "core coupling" terms, in which the boson is absorbed by the core; and gauge terms, in which the boson absorption is coupled to the potential  $V$ . Both of these latter terms can involve transitions from one intrinsic state to another. The different types of terms are easily seen by expanding the absorption reaction to lowest order in the potential  $V$ , as is shown diagrammatically in Fig. 1. The terms in Fig. 1(b) represent inclusion of initial and final-state interactions; the term in Fig. 1(c) represents dispersive corrections, i. e., absorption of a meson while the residual nucleus is in an excited state, Fig. 1(d) shows excitation or deexcitation of the core by coupling to the boson, or what we have called the core coupling terms; Fig. 1(e) illustrates the gauge terms, where the boson couples directly to the potential. For example, if we were considering the reaction  $A(\gamma, N)B$ , then Fig. 1(d) would represent the "semidirect"<sup>7</sup> terms, where the photon couples to intrinsic (e. g., giant resonance) collective states of the residual nucleus, and Fig. 1(e) would represent the "exchange current" terms, where the photon couples to the charge of a virtual exchanged meson.

In general, solving the coupled nuclear equations and calculating the absorption reactions is a formidable task. It is even more complicated for pion absorption reactions, where the pion is both the "external" absorbed meson and an important component of the nuclear force. In this calculation, we wish to make the reaction as simple as possible, so that we can solve analytically for the nuclear wave functions, while still retaining some connection to the underlying physics. In this way, we hope to illustrate the various effects of orthogonality as clearly as possible in a multichannel problem. With this in mind, we make the following simplifications for the purpose of illustration:

(1) We consider only the nucleon transition operator terms in the reaction, i. e., we set  $F_{nn'}(\vec{k}) = 0$

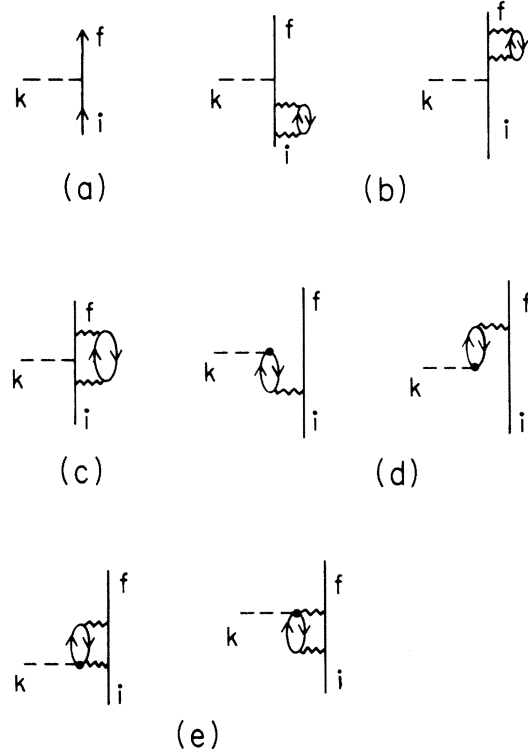


FIG. 1. (a) Lowest-order diagram for absorbing a scalar boson of momentum  $k$  (we have not included the elastic nucleon-core interactions in this diagram). (b) Initial correlations and final-state interactions. (c) Dispersive correction to the absorption amplitude. (d) Core-coupling terms for the absorption. (e) Gauge terms, representing coupling of the boson to the potential. Figure reprinted from Ref. 5(a).

in Eq. (2.5).

(2) We use one-term separable potentials for the interaction  $V$ ,

$$V_{nn'}(\vec{p}, \vec{p}') = \sum_l (2l+1) \lambda^{(l)} v_n^{(l)}(p) v_{n'}^{(l)}(p') P_l(\hat{p} \cdot \hat{p}'). \quad (2.6)$$

In Eq. (2.6),  $V_{nn'}$  is the (nonlocal) potential coupling intrinsic states  $n'$  and  $n$ .  $\lambda^{(l)}$  is a coupling constant,  $v_n^{(l)}(p)$  is a form factor depending upon the magnitude of the momentum  $p$ , and  $P_l$  is the Legendre polynomial of order  $l$ .

With the assumption of separable potentials, we can solve directly for the bound and scattering wave functions. To simplify the resulting algebra even further, we choose a "two-state" system by restricting the core intrinsic states to a "ground state" ( $n=0$ ) and one "excited state" ( $n=1$ ). Our model is then the following: We consider a system in which originally we have a nucleon bound to a nuclear core in an  $s$ -wave orbit. The nucleus ab-

sorbs a boson, leading asymptotically to a free nucleon and the residual nucleus in its ground state. It is easy to show that the single-particle wave functions take the form

$$\psi_n(\vec{p}) = \frac{N v_n^{(0)}(p)}{E_B - E_n(p) - \epsilon_n}, \quad (2.7)$$

$$\begin{aligned} \psi_n^{(-)}(\vec{p}) &= (2\pi)^3 \delta(\vec{p} - \vec{k}_f) \delta_{n,0} \\ &+ \sum_l \lambda^{(l)} \frac{(2l+1)}{D_l(E_-)} \frac{v_n^{(l)}(p) v_0^{(l)}(k_f) P_l(\hat{p} \cdot \hat{k}_f)}{E - E_n(p) - \epsilon_n - i\eta}. \end{aligned} \quad (2.8)$$

In Eq. (2.7),  $E_B$  is the bound-state energy,  $E_n(p)$  is the kinetic energy corresponding to the  $n$ th state,

$$E_n(p) = p^2/2\mu_n,$$

and  $N$  is the normalization factor for the bound state. In Eq. (2.8), the asymptotic momentum of the nucleon is  $\vec{k}_f$ , and  $D_l(E_-) \equiv \lim_{\eta \rightarrow 0^+} D_l(E - i\eta)$  is the Jost function for this interaction. The details of the solutions are given in Appendix A. For separable interactions, we have used the Yamaguchi<sup>8</sup> form factors

$$v_n^{(l)}(p) \sim \frac{p^l}{p^2 + a_{nl}^2}; \quad (2.9)$$

with these form factors, the Jost functions can be calculated analytically. The details of the wave functions and transition matrix elements are given in Appendix B.

Now that we have the nuclear wave functions necessary for our model, we can evaluate the transition matrix element for absorbing a scalar boson of momentum  $\vec{k}$ . For simplicity, and to allow comparison with Noble's calculations for a one-channel potential, we have used the transition operator

$$O = 1e^{\vec{k} \cdot \vec{\tau}}. \quad (2.10)$$

This would correspond to absorbing an undistorted scalar meson of momentum  $\vec{k}$ . With this choice for the transition operator and our assumptions for the nuclear system, Eq. (2.5) takes the form

$$\begin{aligned} T_{fi}(\vec{k}) &= \int \frac{d\vec{p}}{(2\pi)^3} [\psi_0^{(-)*}(\vec{p} + \vec{k}) \psi_0(\vec{p}) \\ &+ \psi_1^{(-)*}(\vec{p} + \vec{k}) \psi_1(\vec{p})]. \end{aligned} \quad (2.11)$$

We can further break this down by noting that Eq. (2.8) can be rewritten as

$$\psi_n^{(-)}(\vec{p}) \equiv (2\pi)^3 \delta(\vec{p} - \vec{k}_f) \delta_{n,0} + \psi_{n,sc}^{(-)}(\vec{p}); \quad (2.12)$$

that is, the scattering wave contains a component of the plane wave in the ground state of the residual nucleus, and scattered spherical waves in all channels. Substituting this into Eq. (2.11) gives

$$\begin{aligned} T_{fi}(\vec{k}) &= \psi_0(\vec{k}_f - \vec{k}) + \int \frac{d\vec{p}}{(2\pi)^3} \psi_0^{(-)*}(\vec{p} + \vec{k}) \psi_0(\vec{p}) \\ &+ \int \frac{d\vec{p}}{(2\pi)^3} \psi_{1,sc}^{(-)*}(\vec{p} + \vec{k}) \psi_1(\vec{p}). \end{aligned} \quad (2.13)$$

The three terms of Eq. (2.13) have a straightforward physical interpretation. The first term of the transition amplitude is what would be obtained by calculating the full bound state wave function, but using a plane wave for the outgoing nucleon. We call this term the PWIA for the reaction. Note that the first and second terms of Eq. (2.13) also include the equivalent of a "spectroscopic factor" for the bound proton wave function. The normalization condition for the full bound state wave function can be rewritten as

$$S \equiv \int \frac{d\vec{p}}{(2\pi)^3} |\psi_0(\vec{p})|^2 = 1 - \int \frac{d\vec{p}}{(2\pi)^3} |\psi_1(\vec{p})|^2. \quad (2.14)$$

Since the single-particle wave function  $\psi_0$  (where the core  $|B\rangle$  is in its ground state) is not normalized to unity, the first term of Eq. (2.13) is equivalent to calculating the transition amplitude using a plane wave for the outgoing proton, but renormalizing the bound wave function to account for the coupling of other nuclear channels.

The first plus second terms of Eq. (2.13) give the transition amplitude for transitions from the bound state leading to the ground state of the residual nucleus but including final-state interactions. In diagrammatic terms, it includes initial and final state interactions such as those shown in Fig. 1(b) to all orders in the potential. In a distorted wave impulse approximation for this reaction, the transition operator would be evaluated between a bound state wave function and a scattering wave function calculated from an optical potential which reproduced the elastic scattering of the nucleon.<sup>9</sup> Since that is just what is given by the first two terms of Eq. (2.13), we denote these two terms as the DWIA for the reaction.

The third term in Eq. (2.13) is a dispersive correction; in this term, the boson is absorbed by the system while the residual system is in its excited state, and the final state interaction eventually takes the nucleus back to its ground state. This corresponds to the graph of Fig. 1(c) calculated to all orders in the potential, and provides the additional contribution to the reaction required by the multichannel nature of the system. It is this additional piece which must be added to the DWIA in order to preserve orthogonality between the bound and scattering states.

For a one-channel potential  $V$ , Noble<sup>5</sup> showed that the final-state interactions  $V$  produced significant cancellations in the transition amplitude rela-

tive to PWIA calculations, which neglected these interactions. In our model, some of the cancellations will be provided by the DWIA amplitudes and some by the dispersive corrections.

In the next section, we will set up three representative models for the nucleon-core interaction, and we will discuss the types of physical systems to which these models correspond.

### III. MODELS FOR TWO-STATE SYSTEMS

We have used separable Yamaguchi potentials for the nucleon-core interaction so that we can solve analytically for the bound and scattering wave functions. With these potentials, the interaction is specified independently for each partial wave. We have chosen  $s$  and  $p$  waves for the nucleon-core scattering, and we assume that the absorption of a boson knocks out a nucleon from an  $s$ -wave bound state. For our calculations, we varied the parameters so as to produce an  $s$ -wave bound state of the nucleon with a binding energy of 30 MeV, and a  $p$ -wave bound state with binding energy of 12 MeV. The excitation energy of the core excited state was chosen to be 30 MeV, and the range of the potentials [see Eqs. (B1) and (B2) in Appendix B] were fixed at 250 MeV/ $c$  for the coupling to the ground state of the core, and 400 MeV/ $c$  for the coupling of the nucleon to the core excited state. We then had two parameters, the strength of the elastic and inelastic interactions, for each partial wave. We have varied the parameters so that they reproduced the same bound state energies but gave rise to three different types of scattering phases. The values of the parameters for these three cases are given in Table I. In Table I we also include the spectroscopic factor  $S$  for the three cases—that is, the square of the normalization of the elastic channel component of the single-particle bound state wave function, given by Eq. (2.14). The closer the spectroscopic factor is to 1, the larger the amplitude of the full wave function relative to the ground state of the residual nucleus.

The first case, which we have called “mostly elastic,” is characterized by a strong coupling of the nucleon to the ground state of the core, and

relatively weak coupling to the core excited state. The elastic coupling parameters  $\alpha_l$  for the  $l$ th partial wave are 3–6 times larger than the corresponding inelastic parameters  $\beta_l$ . The resulting elastic scattering phase shifts for this model are shown in Fig. 2. We can write the  $S$  matrix for elastic scattering of a nucleon from the ground state of the core as

$$S_{00}^{(l)}(E) = \eta_l e^{2i\delta_l}, \quad (3.1)$$

where  $S_{00}^{(l)}$  is the elastic scattering  $S$ -matrix element for partial wave  $l$  and kinetic energy  $E$ ,  $\eta_l$  is the magnitude of the scattering amplitude and  $\delta_l$  is the phase shift. As can be seen from Fig. 2, the magnitude of the elastic scattering amplitude is always relatively close to 1, and the elastic cross section is never less than  $\frac{2}{3}$  of the total cross section for this system. Since the mostly elastic model is characterized by weak coupling to the inelastic channel, we might expect results for knockout reactions in this system to be close to results calculated ignoring the coupling to the inelastic channel.

The second case we have examined is called the “strongly inelastic” case. This is characterized by strong coupling to the excited state of the core. The elastic scattering phases corresponding to these parameters are shown in Fig. 3. Above inelastic threshold, the reaction cross section is large and becomes about twice as large as the elastic cross section.

The third case we have examined is called a “strong absorption” model. This system exhibits very strongly inelastic resonances which are frequently observed in elementary particle reactions (for example, the pion-nucleon phase shifts in the  $D_{13}$  and  $F_{15}$  partial waves). In these coupled systems, there is a very strong attraction producing a resonance in an inelastic channel; in the elastic channel, such a resonance appears as a sharp decrease in the magnitude of  $\eta_l$  and a corresponding rapid change (either increase or decrease) in  $\delta_l$ . In Fig. 4, we show the elastic  $S$ -matrix elements for our strong-absorption case. For the parameters we have chosen, the system displays an  $s$ -

TABLE I. Range and strength parameters for separable interactions, as given in Eqs. (B1) and (B2). Spectroscopic factor  $S$  for each potential as defined in Eq. (2.14).

	Elastic channel		Inelastic channel		Spectroscopic factor
	$\alpha_0$	$\alpha_1$	$\beta_0$	$\beta_1$	
Mostly elastic	3.10	0.87	0.50	0.30	0.922
Strongly inelastic	1.21	0.63	2.20	0.54	0.513
Strong absorption	1.77	0.48	1.70	0.70	0.666
Range	$a = 250$ MeV		$b = 400$ MeV		

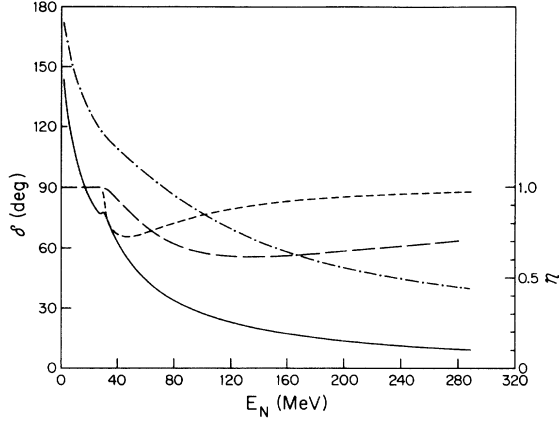


FIG. 2. Elastic scattering phase parameters, defined from Eq. (3.1), vs nucleon kinetic energy (MeV) for the mostly elastic case. Solid curve:  $\delta_0(l=0)$ , in degrees. Dotted curve:  $\delta_1(l=1)$ . Short-dashed curve:  $\eta_0$ . Long-dashed curve:  $\eta_1$ .

wave inelastic resonance at about 40 MeV, and a  $p$ -wave resonance at about 110 MeV. In Fig. 5, we graph the Argand diagram

$$f_i \equiv (\eta_i e^{2i\delta_i} - 1)/2i \quad (3.2)$$

for the strong-absorption case. The resonances are visible as the rapid excursions through the center of the Argand circle, and the form of Fig. 5 is characteristic of strongly inelastic resonances in coupled systems.<sup>10</sup>

The three cases we have chosen are simple enough to solve analytically, but at the same time they exhibit characteristics of more complicated (and hence more realistic) systems. In the next section we will calculate transitions for absorbing a scalar boson and knocking out a nucleon, leading

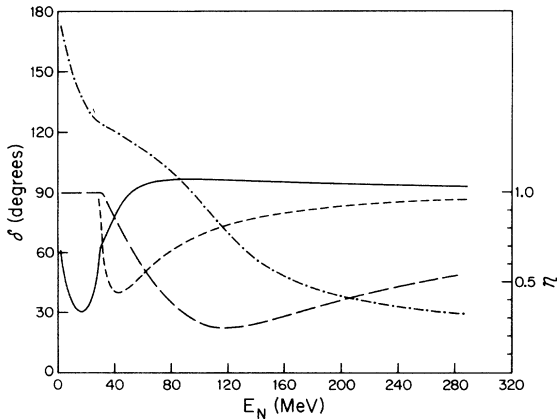


FIG. 3. Elastic scattering phase parameters for the strongly inelastic case. Solid curve:  $\delta_0+90^\circ$ . Other curves are labeled as in Fig. (2).

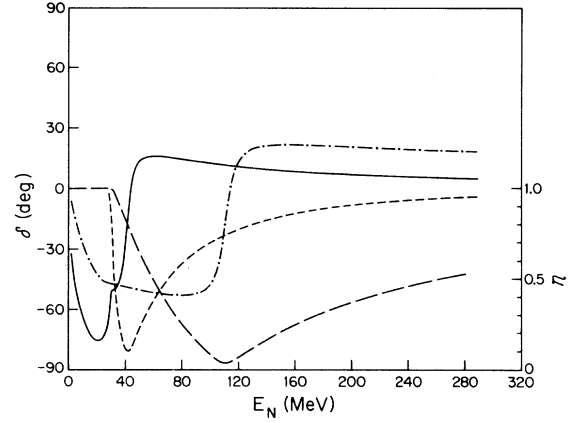


FIG. 4. Elastic scattering phase parameters for the case of strong absorption. Notation is that of Fig. (2).

asymptotically to a state with a free nucleon and the ground state of the core. We will use the nucleon-core coupled wave functions for the three model cases described in this section.

#### IV. RESULTS AND DISCUSSION

In Figs. 6–8, we show the differential cross section  $d\sigma/d\Omega$ , in  $\mu\text{b}/\text{sr}$ , vs c.m. scattering angle  $\theta$ , for the following reactions: a massless scalar boson, with transition operator given by Eq.

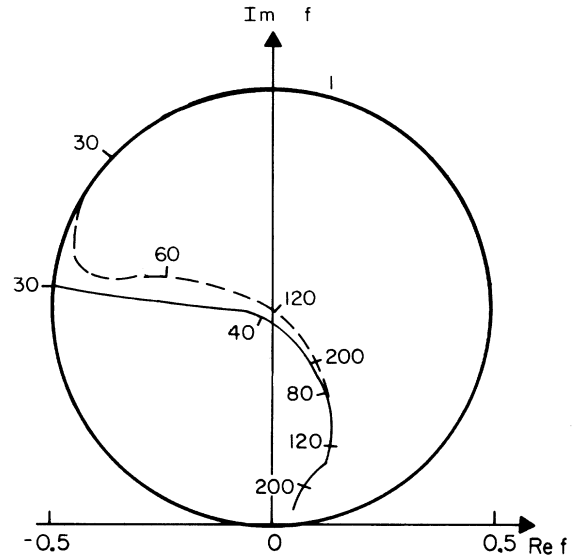


FIG. 5. Argand diagram for the strong absorption phase parameters. Real vs imaginary parts of  $f_i \equiv (\eta_i e^{2i\delta_i} - 1)/2i$ . Solid curve:  $s$  wave. Dashed curve:  $p$  wave. Representative energies are marked off on the diagram; the rapid decrease in magnitude of  $\eta$  and rapid increase in phase occur at the inelastic resonance energies.

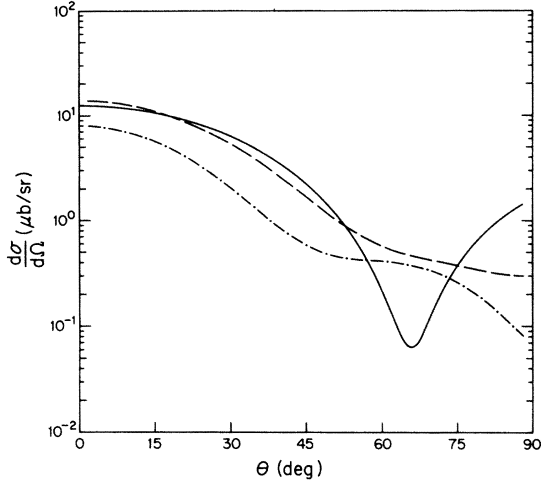


FIG. 6. Differential cross section  $d\sigma/d\Omega$  ( $\mu\text{b}/\text{sr}$ ) vs c.m. scattering angle  $\theta$ , for absorption of a massless scalar boson. The nucleon-nucleus interaction is calculated with the mostly elastic parameters. Solid curve: boson c.m. energy  $E=40$  MeV. Dashed curve:  $E=120$  MeV. Dot-dashed curve:  $E=200$  MeV.

(2.10), is absorbed by the nucleus, knocking out a nucleon and leaving the core in its ground state. In the initial state the ejected nucleon is bound in an  $s$ -wave state with a binding energy of 30 MeV, and we consider  $s$  and  $p$  waves in the final nucleon-nucleus scattering. The solid curves represent absorption cross sections for a scalar boson c.m. energy of 40 MeV, the dashed curve for 120 MeV, and the dot-dashed curve for 200 MeV. Figure 6 gives the results for the case of mostly elastic scattering, as discussed in Sec. III; Fig. 7 gives the results for the strongly inelastic scattering case; and Fig. 8

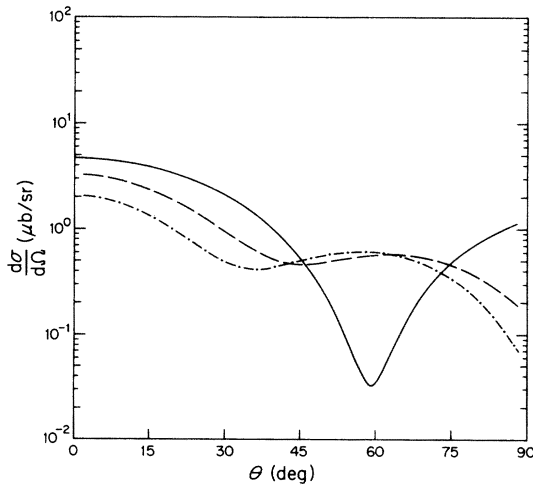


FIG. 7.  $d\sigma/d\Omega$  vs  $\theta_{\text{c.m.}}$  for absorption of a massless scalar boson with the strongly inelastic scattering parameters. Notation is that of Fig. 6.

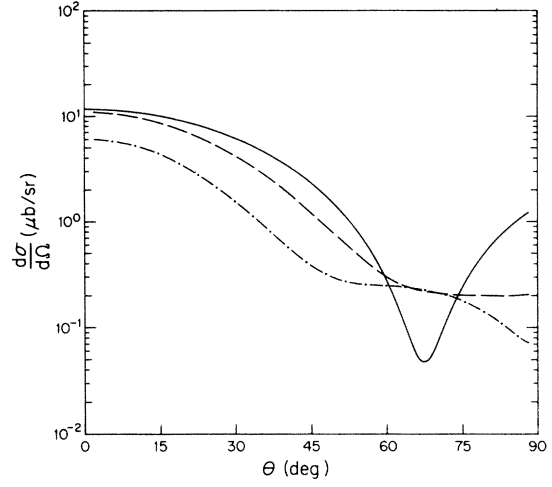


FIG. 8.  $d\sigma/d\Omega$  vs  $\theta_{\text{c.m.}}$  for absorption of a massless scalar boson with the strong absorption scattering parameters. Notation is that of Fig. 6.

represents the case of strong absorption in the nuclear interaction. In all three cases, the  $s$ - and  $p$ -wave final state interaction terms interfere and produce a minimum in  $d\sigma/d\Omega$  at about  $60^\circ$  at 40 MeV, but this minimum is not present in the reaction at higher energies.

We are interested in whether what we have termed the DWIA provides a reasonable fit to the exact knockout amplitude. If the nuclear interaction were a single-channel local interaction  $V(\vec{r})$ , then Noble<sup>5</sup> derived some very useful relations which showed the persistent influence of orthogonality constraints on the transition amplitudes. We will use some of these relations to compare and contrast with our own coupled-channel results, so we recapitulate Noble's arguments here. The results are most easily derived in a coordinate-space representation, where the desired transition amplitude has the form

$$T_{fi}(\vec{k}) = \int d\vec{r} \psi_f^{(-)*}(\vec{r}) e^{i\vec{k}\cdot\vec{r}} \psi(\vec{r}). \quad (4.1)$$

If we insert a plane wave at this point for the outgoing scattered wave with asymptotic momentum  $\vec{k}_f$ , then we obtain

$$T_{P\text{WIA}}(\vec{k}) = \psi(\vec{k}_f - \vec{k}), \quad (4.2)$$

using wave functions which manifestly violate orthogonality. Using the fact that the bound and scattering wave functions are eigenfunctions of the nuclear Hamiltonian  $\mathcal{K}$ , then Eq. (4.1) can be rewritten as

$$T_{fi}(\vec{k}) = \frac{i\vec{k}}{k_f^2 + \kappa^2} \int d\vec{r} \psi_f^{(-)*}(\vec{r}) [\vec{\nabla} - \vec{\nabla}'] \psi(\vec{r}). \quad (4.3)$$

In Eq. (4.3), the binding energy of the single nu-

cleon is  $\kappa^2/2M$ . If we approximate  $\psi_f^{(-)}(\vec{r})$  by a plane wave in Eq. (4.3), and we take the limit of large  $k_f$ , we find the "modified plane-wave" limit

$$[T_{\text{MPW}}(\vec{k})] \approx \frac{2\vec{k} \cdot \vec{k}_f}{k_f^2 + \kappa^2} T_{\text{PWIA}}(\vec{k}), \quad k \ll k_f. \quad (4.4)$$

On the other hand, if we use the "eikonal approximation"

$$\vec{\nabla} \psi_f^{(-)*}(\vec{r}) \approx -i\hat{k}_f [k_f^2 - 2MV(\vec{r})]^{1/2} \psi_f^{(-)*}(\vec{r}), \quad (4.5)$$

then Noble showed that for large  $k_f$

$$T_{\text{EK}}(\vec{k}) \approx \frac{\vec{k} \cdot \vec{k}_f}{k_f^2} T_{\text{PWIA}}(\vec{k}), \quad k \ll k_f. \quad (4.6)$$

The difference of roughly a factor of 2 between the MPW expression of Eq. (4.4) and the eikonal result of Eq. (4.6) points out the importance of the final-state interactions and shows that the correct amplitude will be very sensitive to the inclusion of the final-state interaction. Both of these approximate results indicate that the plane-wave impulse approximation result should give a considerable overestimate of the exact result at all energies.

The previous results have assumed a single-channel potential  $V$ , and the eikonal result has assumed the validity of the "local WKB approximation." Clearly, neither of these approximations is valid for a multichannel reaction with separable interactions for the nuclear potential. Nevertheless, we compare our exact results with these approximations in order to see how the one-channel results are modified by the presence of coupled channels, and also to see whether a distorted-wave calculation will successfully reproduce the exact results, despite the failure of the plane-wave approximation.

From the results of Eqs. (4.4) and (4.6), we see that it is useful to compare the ratio of the plane-wave (and distorted-wave) results with the exact amplitude. In Fig. 9, we graph the ratios of the amplitudes

$$R_{\text{PW}} \equiv |T_{\text{PWIA}}/T| \quad \text{and} \quad R_{\text{DW}} \equiv |T_{\text{DWIA}}/T| \quad (4.7)$$

vs the c. m. momentum of the scalar boson.  $T_{\text{PWIA}}$  is the first term of Eq. (2.13),  $T_{\text{DWIA}}$  is the sum of the first and second terms, and  $T$  is the full amplitude including the dispersive corrections and hence satisfying the orthogonality condition. The results of Fig. 9 are for the mostly elastic scattering parameters. As was predicted by Noble, the PWIA amplitude is considerably larger than the exact result, and the plane-wave result does not approach the exact result at large energies. The distorted-wave result is considerably closer to the exact result; however, the DWIA cross section for this reaction will still be a factor of 2 greater than the exact cross section (which in-

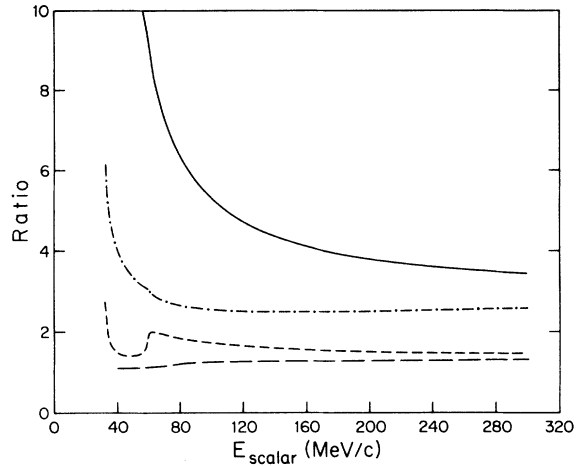


FIG. 9. Ratio of the plane-wave and the distorted-wave approximations to the exact result for the mostly elastic case.  $R_{\text{PW}}$  and  $R_{\text{DW}}$  [see Eq. (4.7)] vs c.m. energy of the scalar boson, for  $\theta_{\text{c.m.}} = 30^\circ$ . Solid curve:  $R_{\text{PW}}$ . Short-dashed curve:  $R_{\text{DW}}$ . Also shown are the same ratios plotted with the monopole term removed from the amplitude. Dot-dashed curve:  $R_{\text{PW}}$  (without monopole). Long-dashed curve:  $R_{\text{DW}}$  (without monopole).

cludes the dispersive corrections). Near the threshold for this reaction, and at the threshold for the opening of the inelastic channel, there are strong energy dependences in the DWIA amplitude relative to the exact result. The calculations shown here (and all further results) are given for a c. m. scattering angle of  $30^\circ$  between the incident boson and the outgoing nucleon; if we repeat the same calculations at  $0^\circ$  we find the discrepancy between the approximate values and the exact result becomes somewhat smaller at all energies, although the qualitative features remain the same at both angles.

In Fig. 10, we compare the ratio  $R_{\text{PW}}$  with the ratios of plane-wave to exact amplitudes estimated by Noble using Eqs. (4.4) and (4.6). We see that the suppression of the plane-wave amplitude is even larger in our model than was predicted by Noble using single-channel forces. However, as seen from Fig. 9, the distorted-wave approximation for this particular case gives reasonably good agreement with the exact result.

In the model which we have used for the scalar boson absorption, a large contribution to the non-orthogonality can come from the monopole part of the meson wave function. Since our absorption operator is just  $O = e^{i\vec{k} \cdot \vec{r}}$  for the meson, we could expand the exponential in a series to obtain

$$T_{fi} = \langle \Psi_f | O | \Psi_i \rangle = \langle \Psi_f | 1 + i\vec{k} \cdot \vec{r} + \dots | \Psi_i \rangle. \quad (4.8)$$

Because of the orthogonality of  $\Psi_f$  and  $\Psi_i$ , the contribution of the "1" term in Eq. (4.8) should give

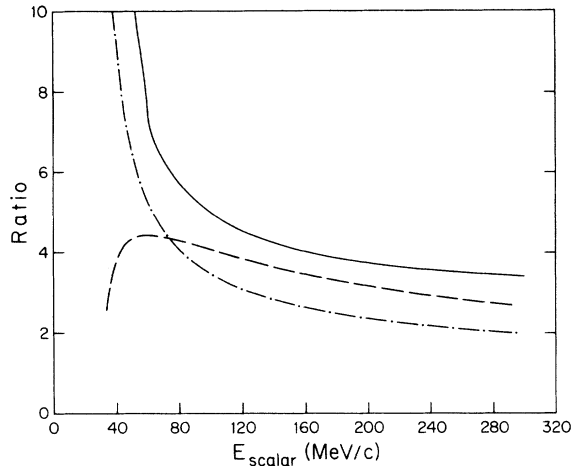


FIG. 10. Ratio of plane-wave approximation to the exact amplitude vs the scalar boson c.m. energy, for  $\theta_{c.m.} = 30^\circ$ . Solid curve:  $R_{PW}$  (includes the monopole contribution). For comparison, the “modified-plane-wave” ratio estimated by Noble [Eq. (4.4)] (dot-dashed curve), and the eikonal ratio [Eq. (4.6)]: the dashed curve.

zero. Consequently, a formally equivalent way of writing  $T_{fi}$  could be obtained by subtracting off the 1 or monopole term, i. e.,

$$T_{fi} = \langle \psi_f | \{ e^{\vec{a} \cdot \vec{r}} - 1 \} | \psi_i \rangle. \quad (4.9)$$

Equation (4.9) is of course identical with (4.8) for properly orthogonalized initial and final states, but using nonorthogonal approximations for the nuclear wave functions will give different results for the two equations. In Fig. 9, we have also plotted the ratios  $R_{PW}$  and  $R_{DW}$  after the monopole term has been removed. We see that removing the monopole part of the transition operator brings the approximate results somewhat closer to the exact results, and in the case of the DWIA approximation it makes the ratio between the approximate and exact results almost independent of energy. In this instance, once we remove the monopole term from the transition amplitude, the ratio between the DWIA amplitude and the exact result is roughly independent of energy. As a consequence, we could adjust the DWIA result to the exact amplitude with an energy-independent renormalization factor.

We have repeated the same knockout calculations for the other two-channel models described in Sec. III. For the parameters which describe the strongly inelastic two-channel model, we have plotted the ratios  $R_{PW}$  and  $R_{DW}$  vs the scalar energy in Fig. 11. For this case, both the plane-wave and distorted-wave amplitudes give a considerable overestimate of the exact result: for large meson energies the distorted wave cross section (which goes as the square of the amplitude) will be a fac-

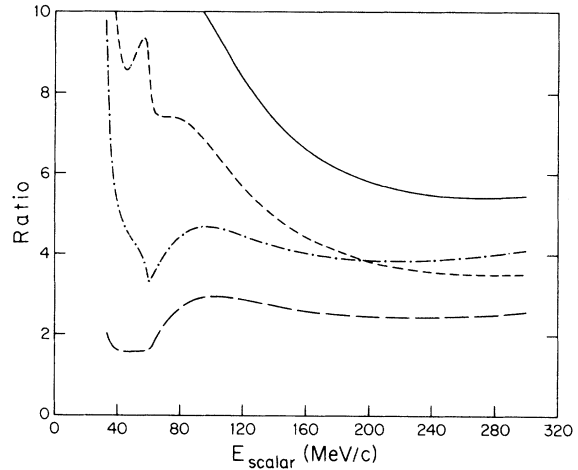


FIG. 11. Ratio of plane-wave and distorted-wave approximation to the exact result for the strongly inelastic scattering parameters. Notation is that of Fig. 9.

tor of 12 greater than the exact result. Removing the monopole part of the transition operator again makes the PW and DW approximations close to energy-independent multiples of the exact results, but both of these approximations give results which are much larger (e. g., factors of 6–15 in the cross sections) than the exact results. In Fig. 12, we compare the ratio  $R_{PW}$  with the one-channel predictions from Noble, and we see that the difference between the plane-wave and exact result is much larger in this particular two-channel case than for the one-channel situation.

For the strong absorption two-channel model, we plot the ratios  $R_{PW}$  and  $R_{DW}$  in Fig. 13. Again, we

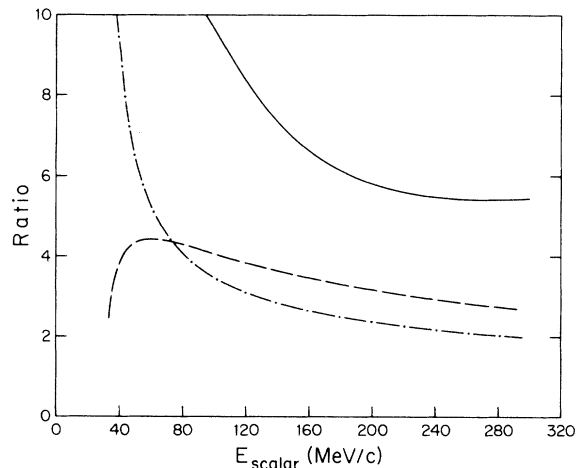


FIG. 12. Comparison of the ratio  $R_{PW}$  of Eq. (4.7) with the ratios estimated by Noble from single-channel considerations. The strongly inelastic parameters are used here, and the notation is that of Fig. 10.

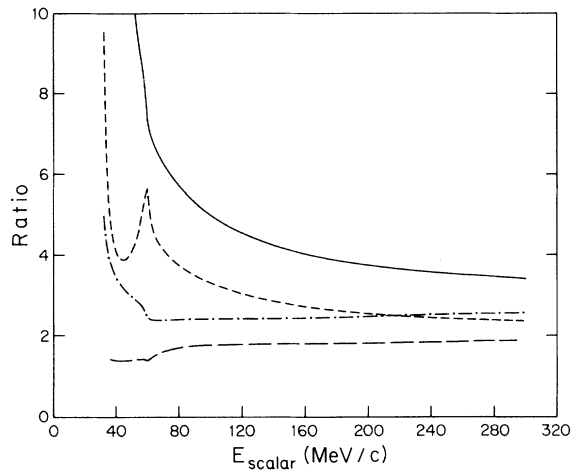


FIG. 13. Ratio of plane-wave and distorted-wave approximations to the exact result for the strong absorption scattering parameters. Notation is that of Fig. 9.

see that both the plane wave and distorted wave approximations seriously overestimate the exact result, and we see that while removing the monopole part of the transition operator takes away the energy dependence of these ratios, the PW and DW approximations are still considerably larger than the actual amplitude.

In all the model calculations shown here we have observed the same qualitative conclusions reached by Noble from considering a one-channel description of knockout reactions: the plane-wave impulse approximation (PW) seriously overestimates the exact result for this reaction, and the discrepancy between the PW and exact results does not improve even for very high energies. In addition, we have been able to compare the exact results for our two-channel model problem with results from an approximation which uses a distorted-wave treatment of the outgoing nucleon together with a spectroscopic factor for the bound nucleon (the DW curves). We find that the DW results are also considerably larger than the exact values, and that these discrepancies also persist even to high energies. Even for the case where the DW results are closest to the exact value (the mostly elastic two-channel model), the DW results still give cross sections at least 40% greater than the exact results. When the monopole part of the transition operator is removed from the amplitudes, then the ratios of the PW and DW approximations to the exact amplitudes are very nearly independent of energy, but the factors needed to renormalize the approximate values to the correct answer are disturbingly large.

Our models are very simple-minded in describing both the transition operator and the complicated particle-nucleus system. However, even these

simple systems may be able to illustrate effects in realistic knockout reactions. We have attempted to choose the parameters in our nucleon-core model in order to simulate effects seen in realistic systems, and we find that the dispersive corrections which would not be included in a standard distorted-wave treatment of knockout reactions might be quite important in determining the overall normalization of these reactions. In our calculations, the dispersive corrections always tended to cancel parts of the DW results, and it was possible to fit the DW results to the exact results with an (approximately) energy-independent renormalization factor: it is not clear whether such qualitative results would also occur in more realistic systems or if they are merely a feature of the specific model we have used.

In our model calculations, dispersive corrections to knockout reactions are large and do not disappear even for high energies of the absorbed boson. Although the calculations shown have been carried out for a massless scalar boson, the qualitative features would be the same if we used a boson of mass 100 MeV but the same transition operator. Our results could be approximately renormalized to the data by multiplying the DWIA amplitude by an energy-independent reduction factor, but this reduction factor would be an *additional* renormalization over and beyond the spectroscopic factor, which has already been included in our model calculations. It might be useful to carry out model calculations for knockout reactions using existing (and more realistic) coupled-channel nuclear reactions codes and simple transition operators, to see whether the large and persistent dispersive corrections which we have obtained are characteristic of such knockout reactions, or whether they are peculiar to the simple two-level models we have employed.

#### ACKNOWLEDGMENTS

The authors would like to thank R. M. Thaler for suggestions and encouragement regarding this work. This research was supported in part by the National Science Foundation.

#### APPENDIX A

In this appendix, we review the solution of equations for constructing continuum and bound state wave functions for coupled systems when simple multichannel separable potentials are used to represent the interactions. We are concerned with the scattering or binding of a nucleon to a core which has an orthogonal spectrum of states by which we represent the  $k$ th excited state as  $|k\rangle$  (the ground state of the core being  $|0\rangle$ ). The full

wave function of the system can then be expanded in the set of states of the core times corresponding single-particle nucleon wave functions relative to the excited state, e. g. ,

$$\langle \hat{\mathbf{p}} | \Psi \rangle = \sum_{\mathbf{k}} \psi_{\mathbf{k}}(\hat{\mathbf{p}}) | k \rangle. \quad (\text{A1})$$

Neglecting center-of-mass effects, the Lippmann-Schwinger equation for the nucleon wave functions is then

$$\psi_{\mathbf{i}} = \varphi_{\mathbf{i}} + G_{\mathbf{i}} V_{i\mathbf{k}} \psi_{\mathbf{k}}; \quad (\text{A2})$$

the Green's function  $G_{\mathbf{i}}$  includes both the relative kinetic energy  $E_{\mathbf{i}}$  of the nucleon and the excitation energy  $\epsilon_{\mathbf{i}}$  of the core. For scattering with an incident plane wave of momentum  $\vec{k}_0$  and a core which is initially in its ground state  $|0\rangle$ , with outgoing scattered waves in all channels, we must solve the coupled equations in momentum representation

$$\begin{aligned} \psi_{\mathbf{i}}^{(+)}(\hat{\mathbf{p}}) &= \varphi_{\mathbf{i}}(\hat{\mathbf{p}}) + \sum_{\mathbf{k}} \int \frac{d\hat{\mathbf{q}}}{(2\pi)^3} \frac{\langle \hat{\mathbf{p}} | V_{i\mathbf{k}} | \hat{\mathbf{q}} \rangle \psi_{\mathbf{k}}^{(+)}(\hat{\mathbf{q}})}{E - E_{\mathbf{i}}(\hat{\mathbf{p}}) - \epsilon_{\mathbf{i}} + i\eta} \\ &\equiv \varphi_{\mathbf{i}}(\hat{\mathbf{p}}) + \sum_{\mathbf{k}} \int \frac{d\hat{\mathbf{q}}}{(2\pi)^3} G_{\mathbf{i}}^{(+)}(p) \langle \hat{\mathbf{p}} | V_{i\mathbf{k}} | \hat{\mathbf{q}} \rangle \psi_{\mathbf{k}}^{(+)}(\hat{\mathbf{q}}). \end{aligned} \quad (\text{A3})$$

For these boundary conditions,  $\varphi_{\mathbf{i}}$  is a plane wave in channel 0;

$$\varphi_{\mathbf{i}}(\hat{\mathbf{p}}) = (2\pi)^3 \delta(\hat{\mathbf{p}} - \vec{k}_0) \delta_{i,0}. \quad (\text{A4})$$

These equations can be straightforwardly solved if we choose a separable potential for the coupling between channels,

$$\langle \hat{\mathbf{p}} | V_{i\mathbf{k}} | \hat{\mathbf{q}} \rangle = \sum_l (2l+1) \lambda_{ij}^{(l)} v_i^{(l)}(p) v_j^{(l)}(q) P_l(\hat{\mathbf{p}} \cdot \hat{\mathbf{q}}). \quad (\text{A5})$$

In Eq. (A5)  $v_i^{(l)}(p)$  is the form factor in the  $l$ th partial wave corresponding to the  $i$ th state of the core, and  $\lambda_{ij}^{(l)}$  is a coupling constant for the inter-

action. For these model calculations the algebra is greatly simplified by setting  $\lambda_{ij}^{(l)} = \lambda^{(l)} \equiv \pm 1$ . The wave functions then obey algebraic equations for each angular momentum state,

$$\psi_{\mathbf{i}}^{(+)}(p) = \varphi_{\mathbf{i}}^{(+)}(p) + \sum_{\mathbf{k}} \lambda^{(l)} v_{\mathbf{i}}^{(l)}(p) G_{\mathbf{i}}^{(+)}(p) I_{\mathbf{k}}^{(l)}, \quad (\text{A6})$$

where

$$I_{\mathbf{k}}^{(l)} = \int \frac{d\hat{\mathbf{q}}}{(2\pi)^3} v_{\mathbf{k}}^{(l)}(q) \psi_{\mathbf{k}}^{(+)}(q). \quad (\text{A7})$$

In order to illustrate the results of our model as simply as possible, we have used a two-level model in which the core has only a ground state and one excited state. This approximation could also be identified with a "doorway" picture, where one assumes that a single intermediate channel or group of states is responsible for connecting the incident channel with more complicated nuclear states. In this case the core levels are restricted to two states, and the algebraic equations are extremely simple. We find that the integrals  $I_{\mathbf{k}}$  of Eq. (A7) are related by

$$I_{\mathbf{k}}^{(l)}(\pm) = \frac{\lambda^{(l)} \Lambda_{\mathbf{k}}^{(l)}(\pm)}{1 - \lambda^{(l)} \Lambda_{\mathbf{k}}^{(l)}(\pm)} I_0^{(l)}(\pm), \quad (\text{A8})$$

where

$$\Lambda_{\mathbf{k}}^{(l)}(\pm) = \int \frac{d\hat{\mathbf{q}}}{(2\pi)^3} [v_{\mathbf{k}}^{(l)}(q)]^2 G_{\mathbf{k}}^{(\pm)}(q) \quad (k=0, 1). \quad (\text{A9})$$

The Jost function for the separable interaction is then given as

$$D_{\mathbf{i}}(E_{\pm}) = 1 - \sum_{\mathbf{k}=0}^1 \lambda^{(l)} \Lambda_{\mathbf{k}}^{(l)}(\pm). \quad (\text{A10})$$

The full scattering wave function then has the form

$$\Psi^{(+)} = \psi_0^{(+)}(\hat{\mathbf{p}}) | 0 \rangle + \psi_1^{(+)}(\hat{\mathbf{p}}) | 1 \rangle, \quad (\text{A11})$$

where

$$\begin{aligned} \psi_0^{(+)}(\hat{\mathbf{p}}) &= (2\pi)^3 \delta(\hat{\mathbf{p}} - \vec{k}_0) + \sum_l (2l+1) \frac{\lambda^{(l)}}{D_{\mathbf{i}}(E_{\pm})} \frac{v_0^{(l)}(p) v_0^{(l)}(k_0) P_l(\hat{\mathbf{p}} \cdot \hat{k}_0)}{E - E_0(p) - \epsilon_0 + i\eta}, \\ \psi_1^{(+)}(\hat{\mathbf{p}}) &= \sum_l (2l+1) \frac{\lambda^{(l)}}{D_{\mathbf{i}}(E_{\pm})} \frac{v_1^{(l)}(p) v_0^{(l)}(k_0)}{E - E_1(p) - \epsilon_1 + i\eta} P_l(\hat{\mathbf{p}} \cdot \hat{k}_0). \end{aligned} \quad (\text{A12})$$

The bound state wave functions are found in a similar fashion by solving the Lippmann-Schwinger equation (A2) with the different boundary conditions. For the bound state,  $\varphi_{\mathbf{i}}(p) = 0$ ; the bound energy  $E_{B, l}$  for a given partial wave is determined by the vanishing of the Jost function for that energy, i. e. ,  $D_{\mathbf{i}}(E_{B, l}) = 0$  for  $D_{\mathbf{i}}$  given by Eq. (A10). Straightforward algebra gives the components of

the bound state wave function as

$$\psi_0^{(l)}(p) = N_l \frac{v_0^{(l)}(p)}{E_{B, l} - E_0(p) - \epsilon_0}, \quad (\text{A13})$$

$$\psi_1^{(l)}(p) = N_l \frac{v_1^{(l)}(p)}{E_{B, l} - E_1(p) - \epsilon_1} \quad (\text{A14})$$

In Eqs. (A13) and (A14) the coefficient  $N_l$  is given

by

$$N_l = \frac{c_l I_0^{(l)}}{1 - \lambda^{(l)} \Lambda_1^{(l)}}, \quad (\text{A15})$$

where  $c_l$  is chosen to normalize the bound state wave function to 1, i. e.,

$$\sum_{\vec{k}} \int \frac{d\vec{p}}{(2\pi)^3} |\psi_{\vec{k}}^{(l)}(\vec{p})|^2 = 1. \quad (\text{A16})$$

#### APPENDIX B

Here, we apply the coupled-channel formalism to calculate the knockout amplitude for the ejection of a nucleon (proton) of momentum  $k_f$  following the interaction of the bound system [proton +  $(A - 1)$  nucleons] with a scalar external probe of momentum  $\vec{k}$ . The  $s$ -wave interactions in the elastic and inelastic channels are taken to be, respectively,

$$v_0^{(0)}(p) = \left( \frac{8\pi a^3 \alpha_0}{2\mu_0} \right)^{1/2} \frac{1}{p^2 + a^2}, \quad (\text{B1})$$

$$v_i^{(0)}(p) = \left( \frac{8\pi b^2 \beta_0}{2\mu_1} \right)^{1/2} \frac{1}{p^2 + b^2}.$$

The corresponding  $p$ -wave interactions are

$$v_0^{(1)}(p) = \left( \frac{8\pi a \alpha_1}{2\mu_0} \right)^{1/2} \frac{p}{p^2 + a^2}, \quad (\text{B2})$$

$$v_i^{(1)}(p) = \left( \frac{8\pi b \beta_1}{2\mu_1} \right)^{1/2} \frac{p}{p^2 + b^2}.$$

Here,  $\{\alpha_i, \beta_i\}$  and  $\{a, b\}$  are the interaction strengths and ranges in the elastic and inelastic channels, respectively. As will be seen in Eqs. (B11) and (B12), the numerical factors are chosen so that the  $\alpha$  and  $\beta$  parameters are dimensionless, and that for the case of a single channel  $\alpha_0 > 1$  ( $\alpha_1 > 1$ ) will guarantee a bound state in the  $l=0$  or  $l=1$  partial waves, respectively.<sup>11</sup> As is well known, the one-term separable potential can produce a maximum of one bound state.  $\mu_0$  is the reduced mass of the nucleon and the recoil particle (mass  $m_R$ ) in the elastic channel and  $\mu_1$  the reduced mass in the inelastic channel (recoil mass  $= m_R + \epsilon_1$ ). We also consider the attractive case so that  $\lambda_{ij}^{(l)} = -1$  with energies  $E = k_f^2/2\mu_0$ ,  $E_{\text{bd}} \equiv \kappa^2/2\mu_0$ , and  $\epsilon_0 = 0$ . For the initial state we take only the  $s$ -wave bound state while for the final scattering state we consider a mixture of  $s$  and  $p$  waves.

For the bound state, a straightforward calculation using contour integrations yields for the normalization constant

$$\frac{1}{N^2} = \frac{2\mu_0 a^2 \alpha_0}{k(k+a)^3} + \frac{2\mu_1 b^2 \beta_0}{k'(k'+b)^3}, \quad (\text{B3})$$

where

$$k'^2 \equiv \frac{\mu_1}{\mu_0} k^2 + Q_1^2$$

and

$$Q_1^2 \equiv 2\mu_1 \epsilon_1.$$

The full amplitude for absorption of a scalar boson of momentum  $\vec{k}$  is given by

$$T_{fi}(\vec{k}; 1) = \int \frac{d\vec{p}}{(2\pi)^3} \{ \psi_0^{(-)+}(\vec{p}) \langle 0 | + \psi_1^{(-)}(\vec{p}) \langle 1 | \} \\ \times \{ \psi_0(\vec{p} - \vec{k}) | 0 \rangle + \psi_1(\vec{p} - \vec{k}) | 1 \rangle \} \\ = \int \frac{d\vec{p}}{(2\pi)^3} \{ \psi_0^{(-)+}(\vec{p}) \psi_0(\vec{p} - \vec{k}) + \psi_1^{(-)+}(\vec{p}) \psi_1(\vec{p} - \vec{k}) \}, \quad (\text{B4})$$

where the  $\psi$ 's are given by Eqs. (A11)–(A14) in Appendix A. The  $(2\pi)^3 \delta(\vec{p} - \vec{k}_f)$  piece in  $\psi_0(\vec{p})$  gives rise to the plane-wave amplitude and is given by

$$T_{\text{PWIA}} \equiv \psi_0(\vec{k}_f - \vec{k}). \quad (\text{B5})$$

The distorted-wave amplitude can be identified as

$$T_{\text{DWIA}} = T_{\text{PWIA}} + T_{\text{DW}},$$

where

$$T_{\text{DW}} \equiv \int \frac{d\vec{p}}{(2\pi)^3} [ \psi_0^{(-)+}(\vec{p}) - (2\pi)^3 \delta(\vec{p} - \vec{k}_f) ] \psi_0(\vec{p} - \vec{k}). \quad (\text{B6})$$

The amplitude  $T_{\text{DWIA}}$  gives the result which we could obtain if we inserted the full elastic wave function  $\psi_0^{(-)+} | 0 \rangle$  for the final state wave function. Thus, if we had an optical potential  $U$  which generated the wave function for elastic scattering of a nucleon from the ground state of the residual nucleus, then  $T_{\text{DWIA}}$  would be the result we obtained by inserting the wave function generated from  $U$  into the knockout amplitude. The full amplitude is obtained by adding an additional dispersive term which represents absorption of the incident particle with the core in its excited state, followed by a nuclear interaction which deexcites the core. We may write this result as

$$T_{fi}(\vec{k}; 1) \equiv T_{\text{DWIA}} + T_{\text{DISP}} = T_{\text{PWIA}} + T_{\text{DW}} + T_{\text{DISP}}, \quad (\text{B7a})$$

where the dispersive correction is given by

$$T_{\text{DISP}} \equiv \int \frac{d\vec{p}}{(2\pi)^3} \psi_1^{(-)+}(\vec{p}) \psi_1(\vec{p} - \vec{k}) \quad (\text{B7b})$$

is the amplitude arising from the inelastic channel.

If we define  $\vartheta$  as the angle between  $\hat{k}_f$  and  $\hat{k}$ , i. e.,  $\hat{k}_f \cdot \hat{k} = \cos \vartheta$ , then a tedious but straightforward calculation, based on the model described above, gives for the amplitudes

$$T_{\text{PWIA}} = \frac{-2\mu_0 N v_0^{(0)} (|\vec{k}_f - \vec{k}|)}{\kappa^2 + (\vec{k}_f - \vec{k})^2}, \quad (\text{B8})$$

$$T_{\text{DW}} = c_0 \int_0^\infty dp \frac{p \ln f_0(p)}{(p^2 + a^2)(p^2 - k_f^2 - i\eta)} \\ + c_1 \cos\theta \int_0^\infty dp \frac{p^2 \ln f_1(p)}{(p^2 + a^2)(p^2 - k_f^2 - i\eta)}$$

$$T_{\text{DISP}} = d_0 \int_0^\infty \frac{dp p \ln g_0(p)}{(p^2 + b^2)(p^2 - \kappa_1^2 - i\eta)} \quad (\text{B9})$$

$$+ d_1 \cos\theta \int_0^\infty dp \frac{p^2 \ln g_1(p)}{(p^2 + b^2)(p^2 - \kappa_1^2 - i\eta)}, \quad (\text{B10})$$

where

$$\kappa_1^2 \equiv \frac{\mu_1}{\mu_0} k_f^2 - Q_1^2,$$

$$c_0 = \frac{-4N(a^3 \alpha_0^3 \mu_0 / \pi)^{1/2}}{D_0(k_f) k (k_f^2 + a^2) (\kappa^2 - a^2)},$$

$$c_1 = \frac{-12Na^2 \alpha_1 k_f (a \alpha_0 \mu_0 / \pi)^{1/2}}{D_1(k_f) k (k_f^2 + a^2) (\kappa^2 - a^2)}, \quad (\text{B11})$$

$$d_0 = \frac{-4Nb^3 \beta_0 \mu_1 [a^3 \alpha_0 / (\pi \mu_0)]^{1/2}}{D_0(k_f) k (k_f^2 + a^2) (k'^2 - b^2)},$$

$$d_1 = \frac{-12Nb^2 \mu_1 k_f [a \alpha_1 \beta_1 \beta_0 / (\pi \mu_0)]^{1/2}}{D_1(k_f) k (k_f^2 + a^2) (k'^2 - b^2)},$$

$$f_0(p) = \frac{\{(p+k)^2 + a^2\} \{(p-k)^2 + \kappa^2\}}{\{(p-k)^2 + a^2\} \{(p+k)^2 + \kappa^2\}}, \\ f_1(p) = \frac{\{(p+k)^2 + b^2\} \{(p-k)^2 + k'^2\}}{\{(p-k)^2 + b^2\} \{(p+k)^2 + k'^2\}}, \quad (\text{B12}) \\ g_0(p) = \left\{ \frac{(p+k)^2 + a^2}{(p-k)^2 + a^2} \right\}^\alpha \left\{ \frac{(p-k)^2 + \kappa^2}{(p+k)^2 + \kappa^2} \right\}^\beta, \\ g_1(p) = \left\{ \frac{(p+k)^2 + b^2}{(p-k)^2 + b^2} \right\}^\gamma \left\{ \frac{(p-k)^2 + k'^2}{(p+k)^2 + k'^2} \right\}^\delta,$$

and

$$\alpha = (p^2 + k^2 + a^2) / (2pk), \\ \beta = (p^2 + k^2 + \kappa^2) / (2pk), \\ \gamma = (p^2 + k^2 + b^2) / (2pk), \\ \delta = (p^2 + k^2 + k'^2) / (2pk). \quad (\text{B13})$$

The Jost functions are found to be

$$D_0(k_f) = 1 - \frac{\alpha_0 a^2}{(a - ik_f)^2} - \frac{\beta_0 b^2}{(b - i\kappa_1)^2} \quad (\text{s wave}), \quad (\text{B14})$$

$$D_1(k_f) = 1 - \frac{\alpha_1 a(a - 2ik_f)}{(a - ik_f)^2} - \frac{\beta_1 b(b - 2i\kappa_1)}{(b - i\kappa_1)^2} \quad (\text{p wave}). \quad (\text{B15})$$

The integrals in Eqs. (B9) and (B10) can further be reduced by using the principal value technique

$$\frac{1}{E + H_0 \pm i\eta} = \frac{P}{E - H_0} \mp i\pi \delta(E - H_0). \quad (\text{B16})$$

This gives [making use of the fact that  $\int_0^\infty dp / (p^2 - k^2) = 0$ ]

$$T_{\text{DW}} = c_0 \left\{ \int_0^\infty \frac{dp}{(p^2 - k_f^2)} \left[ \frac{p \ln f_0(p)}{(p^2 + a^2)} - \frac{k_f \ln f_0(k_f)}{(k_f^2 + a^2)} \right] + \frac{i\pi \ln f_0(k_f)}{2(k_f^2 + a^2)} \right\} \\ + c_1 \cos\theta \left\{ \int_0^\infty \frac{dp}{(p^2 - k_f^2)} \left[ \frac{p^2 \ln f_1(p)}{(p^2 + a^2)} - \frac{k_f^2 \ln f_1(k_f)}{(k_f^2 + a^2)} \right] + \frac{i\pi k_f \ln f_1(k_f)}{2(k_f^2 + a^2)} \right\}, \quad (\text{B17})$$

$$T_{\text{DISP}} = d_0 \left\{ \int_0^\infty \frac{dp}{(p^2 - \kappa_1^2)} \left[ \frac{p \ln g_0(p)}{(p^2 + b^2)} - \frac{\kappa_1 \ln g_0(\kappa_1)}{(\kappa_1^2 + b^2)} \right] \theta(\kappa_1^2) + \frac{i\pi \ln g_0(\kappa_1)}{2(\kappa_1^2 + b^2)} \theta(\kappa_1^2) \right\} \\ + d_1 \cos\theta \left\{ \int_0^\infty \frac{dp}{(p^2 - \kappa_1^2)} \left[ \frac{p^2 \ln g_1(p)}{(p^2 + b^2)} - \frac{\kappa_1^2 \ln g_1(\kappa_1)}{(\kappa_1^2 + b^2)} \right] \theta(\kappa_1^2) + \frac{i\pi \kappa_1 \ln g_1(\kappa_1)}{2(\kappa_1^2 + b^2)} \theta(\kappa_1^2) \right\}; \quad (\text{B18})$$

in Eq. (B18),  $\theta(x)$  is the Heaviside step function

$$\theta(x) = \begin{cases} 1 & x > 0 \\ 0 & x < 0. \end{cases}$$

For numerical calculations, we consider the following three cases: (a) mostly elastic, (b) strongly inelastic, and (c) strong absorption for each of the following scalar masses: (i) 0 MeV, (ii) 100

MeV. We have not plotted the results for a scalar mass of 100 MeV, but they are qualitatively the same as the results for the massless case. The potential parameters used for the three cases are listed in Table I. The inelastic channel excitation energy  $\epsilon_1$  and the nucleon binding energy were both fixed at 30 MeV. The integrations were done numerically using Gaussian integration.

\*Present address: Department of Physics, University of Southern Illinois, Carbondale, Illinois 62901.

- <sup>1</sup>D. F. Measday and G. A. Miller, *Ann. Rev. Nucl. Part. Sci.* 29, 121 (1979), and references therein.
- <sup>2</sup>J. L. Matthews, in *Nuclear Physics with Electromagnetic Interactions*, Lecture Notes in Physics No. 108, edited by H. Arenhövel and D. Drechsel (Springer, Berlin, 1979), p. 369 and references therein.
- <sup>3</sup>V. I. Kukulín and V. N. Pomerantsev, *Ann. Phys. (N.Y.)* 111, 330 (1978), and references therein.
- <sup>4</sup>R. R. Scheerbaum, C. M. Shakin, and R. M. Thaler, *Ann. Phys. (N.Y.)* 76, 333 (1973).
- <sup>5</sup>(a) J. V. Noble, *Phys. Rev. C* 17, 2151 (1978); (b) J. M. Eisenberg, J. V. Noble, and H. J. Weber, *ibid.* 19, 276 (1979); (c) J. V. Noble (unpublished).
- <sup>6</sup>H. Feshbach, *Ann. Phys. (N.Y.)* 5, 357 (1958); 19, 287

(1962).

- <sup>7</sup>G. E. Brown, *Nucl. Phys.* 57, 339 (1964).
- <sup>8</sup>Y. Yamaguchi, *Phys. Rev.* 95, 1628 (1954).
- <sup>9</sup>N. Austern, *Direct Reaction Nuclear Theories* (Wiley, New York, 1970).
- <sup>10</sup>In most resonance cases, the Argand diagram displays a loop or circle which is correlated with the resonance. For this particular case, the presence of bound states for both  $l=0$  and  $l=1$  means that the phase shift begins by decreasing rapidly, and then it increases at the resonance energy. The resulting phase behavior does not show a "loop" in the Argand plot but is nevertheless indicative of a resonance in the coupled system.
- <sup>11</sup>The conditions for existence of a bound state in the coupled-channel system are  $\alpha_0 + \beta_0 b^2 / (b + Q_1)^2 \geq 1$  for  $l=0$ ,  $\alpha_1 + b\beta_1(b + 2Q_1) / (b + Q_1)^2 \geq 1$  for  $l=1$ .